Double Gamma Decay in $^{40}Ca^{\dagger}$

E. Beardsworth,* R. Hensler, J. W. Tape,‡ N. Benczer-Koller, and W. Darcey§
Physics Department, Rutgers University, New Brunswick, New Jersey 08903

and

Jack R. MacDonald¶
Bell Telephone Laboratories, Murray Hill, New Jersey 07974
(Received 16 February 1973)

A positive indication of double γ decay in ^{40}Ca may have been observed. A branching ratio $\Gamma_{\gamma\gamma}/\Gamma = (3.3^{+0.5}_{-1.2}) \times 10^{-4}$ is reported for the decay of the 3.35-MeV 0_2^+ state. The state was preferentially populated by the (p, p') reaction at a bombarding energy of 5.08 MeV, through a resonance in the compound nucleus ^{41}Sc. Recoil particles were detected in an annular detector at 180°, and γ rays were detected in two NaI(Tl) detectors at 45° and 135° with respect to the beam axis. Triple time coincidence was demanded of the three radiations, and γ-energy signals were event recorded, together with coincidence information, permitting subsequent generation of two-dimensional energy spectra (E_{γ_1} vs E_{γ_2}) for real, correlated random, and random coincidences. The distribution of double-γ events was analyzed by the maximum-likelihood technique and was found to be consistent with the assumption of ($E1$, $E1$) multipolarities. A variety of background processes was considered, but none was found likely to account for the observed spectrum. A brief historical review is given, along with a summary of previous experiments which sought to observe double γ decay in ^{40}Ca and other nuclei. Existing theories for the process are examined.

I. INTRODUCTION

The decay of an excited state of an atom or nucleus by the simultaneous emission of two photons is an allowed, second-order quantum-mechanical process wherein the two photon energies sum to the full transition energy, with each photon giving rise to a continuum energy spectrum whose shape is determined by the properties of the system. First-order processes, when allowed, usually dominate the decay by several orders of magnitude. In cases where first-order processes are forbidden or severely retarded (by selection rules, for example), two-photon emission may be significant.

Two-photon transitions in atoms were first treated in detail by Goeppert-Mayer[1] in 1931, who set forth the necessary formalism, and pointed out the close relation to the Raman effect. In 1940, Breit and Teller[2] calculated that double-photon emission would limit the lifetime of metastable states of interstellar hydrogen and helium. The first experimental evidence for two-photon transition was obtained in 1950, for the case of absorption. Hughes and collaborators[3] describe a variety of experiments showing absorption at one half the energy of an (otherwise forbidden) transition, the first of which was in the electric quadrupole spectrum of ^{85}RbF. Decay was not observed until 1968, when Elton, Palumbo, and Greim[4] reported seeing the continuum radiation from the two-photon decay of the metastable 2^1S state in helium-like neon IX.

In an early reference to nuclear double γ decay, Oppenheimer and Schwinger,[5] in considering a suggestion that the first excited state of ^{16}O might have spin and parity 0^+, pointed out the possibility of double γ decay and the experimental difficulty of observing such a process in competition with the dominant pair decay. In an attempt to explain nuclear isomerism, Sachs[6] proposed that the ground and excited states might have zero spin and opposite parity, in which case double γ emission would be amongst the most probable modes of decay. Several experimental searches have been made for double γ decay of isomeric states (see Ref. 7), three of which were successful. Two-photon decay in competition with $M4$ transitions has been observed by Alväger and Ryde[8] and Fischbeck and Abdulla[9] in the case of $^{131}Xe^m$, and by Beusch[10] in $^{137}Ba^m$. The observed ratios of two- to one-photon decay are 2.0×10^{-3} and 6.4×10^{-4}, respectively.

Several attempts have been made to observe double γ decay of the first excited 0^+ states of ^{16}O, ^{40}Ca, and ^{90}Zr. In these cases, first-order electromagnetic decay processes are strictly forbidden and decay proceeds dominantly by internal conversion and/or pair emission. Several authors have reported observation of positive effects in ^{16}O and ^{90}Zr with indicated branching ratios in conflict with upper limits set by other experiments. The results of these experiments are summarized in Table I.

The major problem associated with these experiments is that of detecting two γ rays, each with a continuous energy distribution, in the presence of a high radiation flux due to the dominant decay mode and various background processes. The sum-coincidence technique has been widely used to provide partial discrimination against competing processes by utilizing the time-coincidence and energy-sum properties which characterize a double-γ-decay event. Two-dimensional analysis of the two γ-ray energies permits examination of the continuum yield, while maintaining the discrimination afforded by the sum-coincidence technique. Further identification of events of interest is obtained by imposing a third coincidence requirement between exciting and decay radiations, which may significantly reduce extraneous radiations at the expense of a much reduced data-collection efficiency.

In all attempts to observe double γ decay of the 3.35-MeV state of ^{40}Ca, the state has been populated by inelastic proton scattering (as in the present experiment). Steady progress has been made in reducing the measured upper limit for the branching ratio:

$$R = \Gamma_{\gamma\gamma}/(\Gamma_\pi + \Gamma_e).$$

(In the case of ^{40}Ca the pair decay is dominant.) The early experiment by Nessin, Kruse, and Eklund[17] involved counting γ-γ coincidence events where each of the γ energies was restricted to the range 1.47–1.87 MeV (that is, a region centered at half the excitation energy). A limit $R < 6\times10^{-3}$ was set. Sutter[19] was the first to employ triple coincidence, and by examining proton energy spectra for various coincidence conditions was able to set the limit at $R < 2.1\times10^{-3}$. Harihar, Ullman, and Wu,[22] in the most recent effort, used the $\gamma\gamma$ sum-coincidence technique augmented by window requirements on each of the γ energies. They report a limit of $R < 4.0\times10^{-4}$ based on an estimate of the number of double γ events that might be present at 3.35 MeV in the sum spectrum.

The present paper reports on a search for the two-photon decay of the 3.35-MeV (0_2^+) state of ^{40}Ca using a triple-coincidence technique coupled with two-dimensional analysis of the 2-γ energy spectra.

II. EXPERIMENTAL APPARATUS AND TECHNIQUE

A. Excitation of the State

The 0_2^+ state at 3.35 MeV in ^{40}Ca was populated by inelastic proton scattering at a proton bombarding energy of 5.087 MeV (Fig. 1). At this energy, a 12.1-keV-wide resonance is observed corresponding to the formation of the 6.045-MeV ($\frac{3}{2}^-$) state in ^{41}Sc. This state proton decays to the 0_2^+ state in ^{40}Ca, thus providing a favorable ratio of inelastic to elastic scattering in comparison with other bombarding energies.[24,25] The relatively low proton bombarding energy of 5.08 MeV had the further advantage of minimizing production of high-energy γ rays due to deexcitation of the 3.737- and 3.904-MeV states in ^{40}Ca, as well as the 4.43-MeV level in ^{12}C, potentially troublesome because of the possibility of "cross talk" between the NaI detectors.

A thin, self-supporting ^{40}Ca metal target was prepared by vacuum evaporation of isotopically enriched (99.995%) ^{40}Ca onto a Formvar-coated Havar foil. After evaporation, the foil was transferred to an argon-atmosphere glove box and placed in a highly anhydrous solvent (chloroform

TABLE I. Summary of previous results for the branching ratio of double γ decay in 0^+-0^+ transitions.

^{16}O	^{40}Ca	^{90}Zr	Investigators	Reference
		$<1.0\times10^{-4}$	Sunyar and Schwarzschild (1959)	11
	$<1.4\times10^{-2}$		Dell *et al.* (1961)	12
$<6.0\times10^{-3}$	$<7.0\times10^{-3}$	$<1.4\times10^{-3}$	Gorodetzky *et al.* (1961)	13
$=2.5\times10^{-3}$			Gorodetzky *et al.* (1961)	14
		$=2.3\times10^{-3}$	Langhoff and Hennies (1961)	15
		$=1.1\times10^{-3}$	Ryde *et al.* (1961)	16
	$<6.0\times10^{-3}$		Nessin *et al.* (1961)	17
		$<4.2\times10^{-4}$	Ryde *et al.* (1963)	18
$=(2.5\pm1.1)\times10^{-3}$	$<2.1\times10^{-3}$	$<8.8\times10^{-4}$	Sutter (1963)	19
$<1.1\times10^{-4}$			Alburger and Parker (1964)	20
		$(<8\times10^{-5})$	Vanderleeden and Jastram (1965)	21
	$<4.0\times10^{-4}$	$<1.8\times10^{-4}$	Harihar *et al.* (1970)	22
		$<1.2\times10^{-4}$	Vanderleeden and Jastram (1970)	7
		$=(5.1\pm2.5)\times10^{-4}$	Nakayama (1972)	23
	$=(3.3^{+0.5}_{-1.2})\times10^{-4}$		Present work	

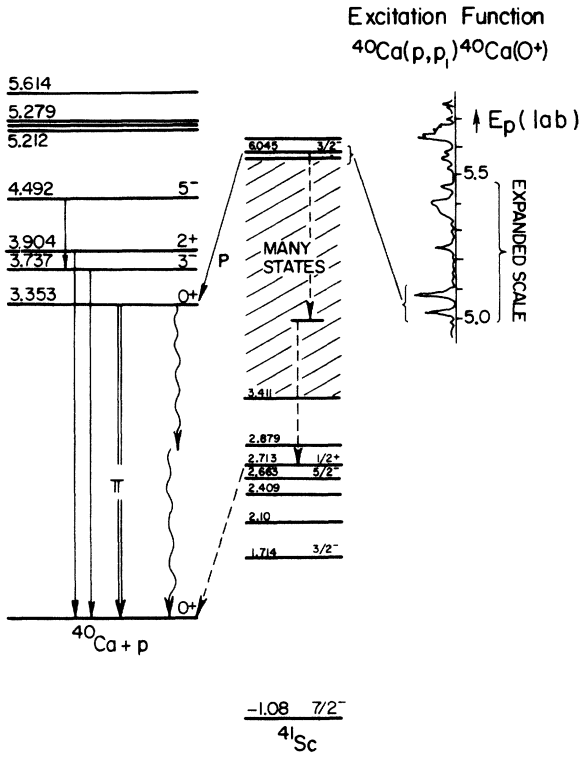

FIG. 1. Level diagram and decay scheme, showing the levels of the compond nucleus and an excitation function for the reaction of interest. The dotted line is discussed in the text.

freshly distilled over magnesium shavings) to dissolve the Formvar. The Ca evaporant was then coaxed onto a frame and secured with wax. Subsequent surface contamination was minimized by storage and transfer to the scattering chamber under vacuum. The resultant target was 0.3 mg/cm^2 thick, assuring optimum utilization of the 12-keV-wide compound resonance.

B. Technique

An event of interest is characterized by a triple coincidence of a proton exciting the state of interest, and two decay γ rays. For any such event, the γ energies were "event recorded," together with coincidence timing information. The requirement that the two γ-ray energies must sum to 3.35 MeV was imposed during subsequent analysis, where the continuum nature of the yield could be examined as well.

A combination of fast and slow, and overlap and TAC (time-to-amplitude converter) timing techniques was utilized for the triple-coincidence determination. Five kinds of events are to be anticipated (see Fig. 2):

(1) bonafide reals, $[p\gamma_1\gamma_2]$;

(2)–(4) doubly-correlated random coincidences, $[p\gamma_1]\gamma_2$, $[p\gamma_2]\gamma_1$, $p[\gamma_1\gamma_2]$;

(5) triple randoms, $[p][\gamma_1][\gamma_2]$.

Entities in brackets are defined to have come from the same single physical event; those outside are

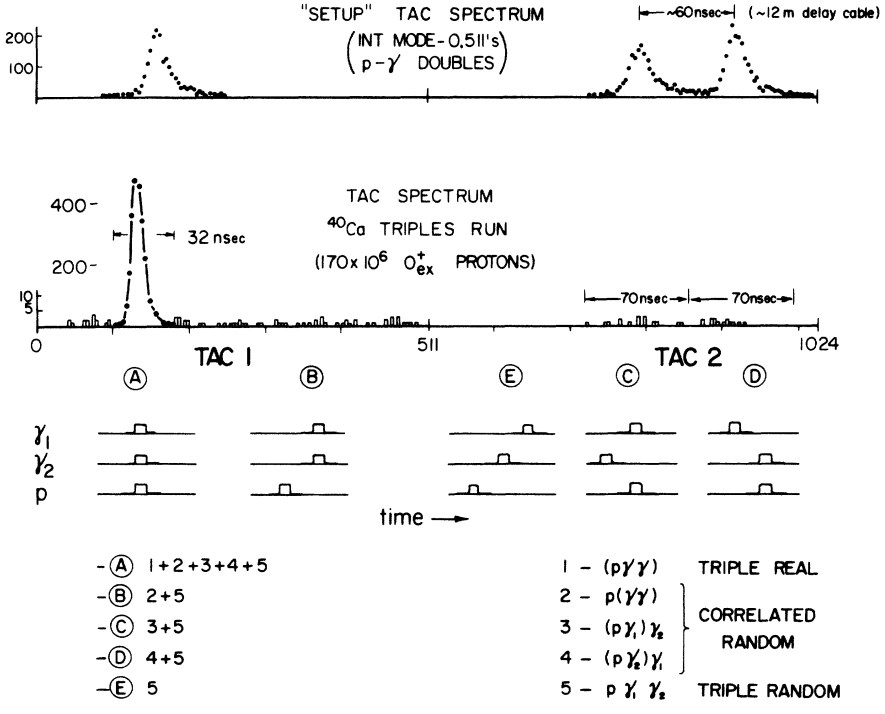

FIG. 2. Representative TAC spectrum, showing regions which correspond to the various kinds of triple coincidences.

from another event and are randomly in coincidence with the event in brackets.

Any coincidence logic used to distinguish type (1) events will not exclude events of types (2)–(5) [event types (2)–(4) will in turn contain type (5)]. The configuration of this experiment permitted the direct, continuous, and simultaneous measurement of each event type.

C. Detectors

Protons scattered near 180° were detected in a 300-mm², 500-μm annular surface-barrier detector located at the entrance to the scattering chamber as shown in Fig. 3. The proton beam from the Rutgers-Bell FN tandem Van de Graaff accelerator was focused through the detector and stopped in a Faraday cup 2 m beyond. A tantalum shield protected the back of the detector from the beam, and aluminized Mylar foil, 6.4 μm thick, covered the front to stop low-energy electrons and α particles. The active surface of the detector was 2.7 cm from the target, thus subtending a solid angle of 0.39 sr.

γ rays were detected in two 12.7×12.7-cm NaI(Tl) crystals located 8.2 cm from the target, in the horizontal plane, at 45 and 135°, respectively, to the beam axis (Fig. 3). This configuration ($\theta_{\gamma\gamma}=90°$) was chosen to minimize coincidence events due to annihilation of the positrons from the predominant pair decay, which gives rise to pairs of 0.511-MeV quanta emerging at 180° to one another. Although an additional measurement at $\theta_{\gamma\gamma}=180°$ would have, in principle, checked the predicted angular correlation of the two decay γ rays, completely different experimental conditions would obtain.

As the electrons and positrons from the pair decay have on the order of 1 MeV (2.3 MeV maximum) kinetic energy, shielding (0.25 mm tantalum and 0.64 cm Lucite) was placed in the scattering chamber to stop them well away from the NaI crystals, thus reducing the number of detected bremsstrahlung events.

D. Electronics

A block diagram of the electronics is shown in Fig. 4. Fast signals for each of the γ rays were taken directly from the photomultiplier anodes and slow energy signals from the tenth dynode were fed to preamplifiers. The fast-particle signal was obtained from a high-input-impedance preamplifier[26] and the slow signal from a charge sensitive field-effect-transistor (FET) preamplifier.[27]

All fast signals were further amplified and then fed to fast differential discriminators to obtain fast-logic timing signals. Crude energy selection by these devices reduced the count rates of signals

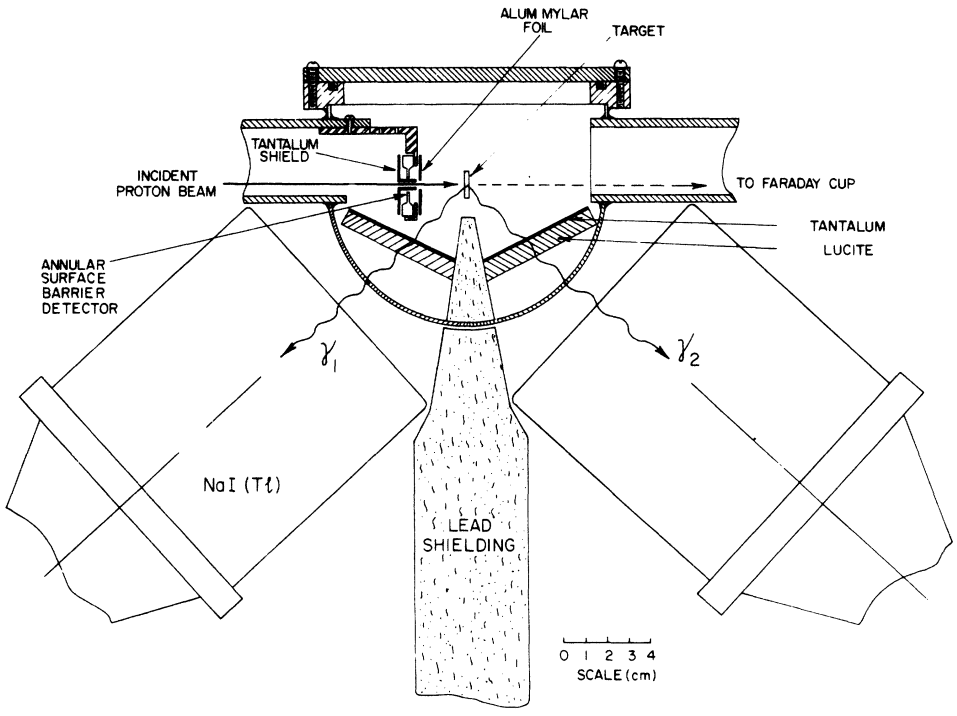

FIG. 3. Scattering chamber and detectors.

fed to the coincidence electronics, by removing signals due to elastically scattered particles and γ rays of energy $\lesssim$0.7 MeV. In particular, this eliminated all events involving the copious 0.511-MeV γ rays.

The particle timing signal was used to "start" each of two time-to-amplitude converters (TAC1 and TAC2). In order to establish the time correlations between γ_1 and γ_2, their timing signals (of width 18.5 nsec) were input to two overlap coincidence circuits (OL1 and OL2). An output from OL1 indicated a γ-γ real coincidence. The second γ signal was delayed through a 12-m cable for input to OL2. An output from OL2 thus indicated a γ-γ random coincidence. The outputs of the two overlap circuits were used to stop TAC1 and TAC2, respectively. Distinct regions of these TAC spectra were then attributable to the various types of events described above (see Fig. 2).

Slow coincidence circuitry (~1 μsec) was used to combine the particle-energy requirement with the fast-logic coincidence determination. Analog signals were suitably shaped and amplified for pulse-height analysis. To establish the particle-energy "window," the proton analog signal was set to a single-channel analyzer (SCA) through a linear gate, which was "enabled" by the fast particle discriminator, thus reducing count rate so as to avoid dead time in the SCA. The total particle count rate was ~45×10^3/sec, but was lowered to ~4.4×10^3/sec by the "fast" energy window.

Two SCA's used in the discriminator mode gave positive logic signals for any output from each of the TAC's, which, together with the particle SCA output, were fed to a slow overlap coincidence matrix.[27] A multiplexer[28] provided fan-in of the two TAC analog signals with appropriate routing, and a master event gate, consisting of the "exclusive OR" of gates fed to it from the slow coincidence circuit.

The γ-ray energy signals (γ_1 and γ_2) and the TAC analog signals were analyzed in three 50-MHz 4096-channel analog-to-digital converters[29] (ADC) interfaced[30] to the Rutgers-Bell Sigma 2 computer, which was programmed in an event-recording configuration. The master event gate instructed the computer to read and store the contents of the ADC's. Preliminary data sorts could be made, providing live display spectra, as defined by the user, to monitor progress of the experiment, while all events were written on magnetic tape.

Scalers were used to monitor discriminator count rates, the γ-γ coincidence circuits, and the "slow" logic, as well as to record elapsed time,

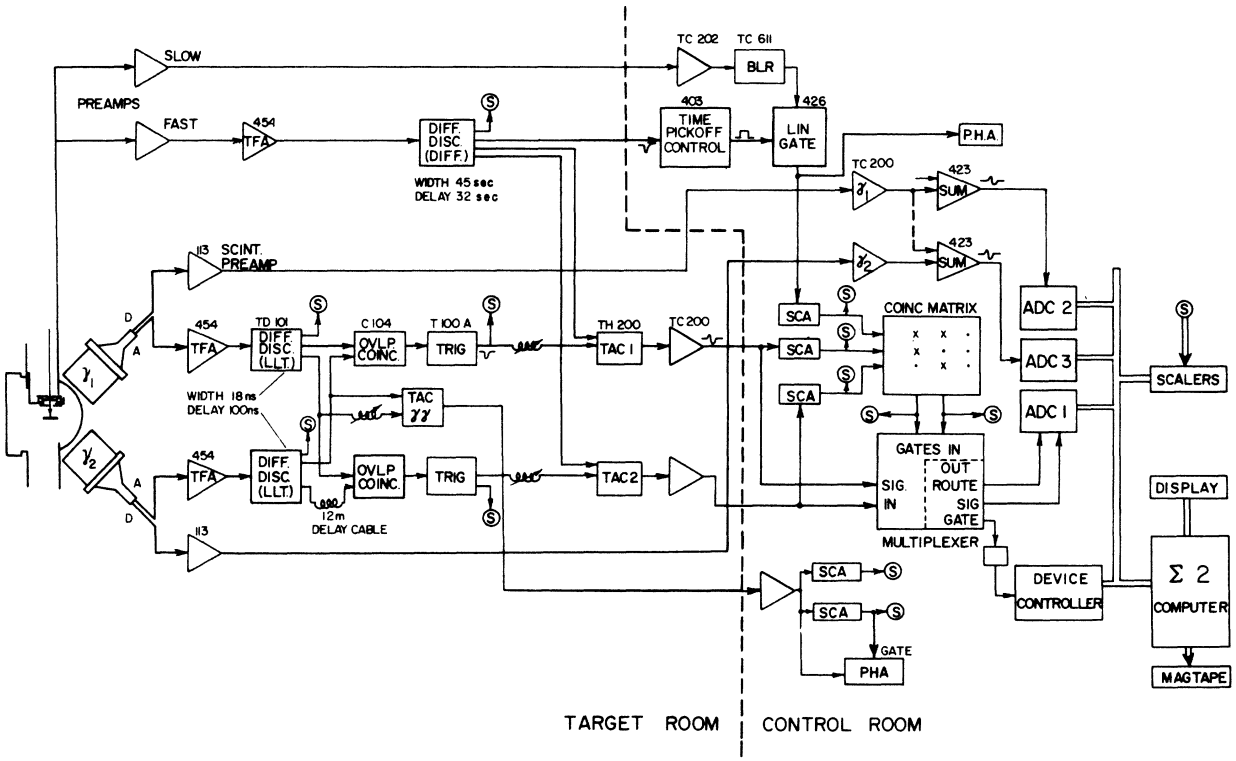

FIG. 4. Block diagram of the electronics.

integrated beam current, and the total number of excitations of the state of interest, as given by the particle SCA output.

E. Procedures

^{40}Ca triple-coincidence data were taken in 6- to 12-h segments, interspersed with checks on γ-ray energy calibrations and the proton-energy-window position. Prior to and following the triple runs, auxiliary spectra were obtained under a variety of coincidence conditions. Individual γ-ray spectra were taken for each crystal in double coincidence with protons exciting the 3.35-MeV state ($p\gamma$ doubles). Also, a short event-recorded run was made of γ-γ doubles. The efficiency measurement described below was done both before and after all ^{40}Ca measurements.

III. AUXILIARY MEASUREMENTS

A. Efficiency Calibration

The functioning of the entire data-acquisition and analysis system was checked, and the over-all detection efficiency was directly measured, by observing a cascade deexcitation of the 3.53-MeV (0^+) state in ^{58}Ni. This state decays 100% by emission of a 2.077-MeV γ ray to the 1.454-MeV (2^+) state, which then decays 100% to the ground state.[31] The cascade has nearly the same sum energy as the double γ decay, and, conveniently, the energies of the two quanta are each close to one half the total transition energy. The 0-2-0 γ-γ angular correlation was taken into account in the analysis.

Double-coincidence (p-γ) measurements were performed for each crystal to determine their individual photopeak efficiencies at representative energies. From the results of these double-coincidence measurements, a triple-coincidence efficiency can be predicted. The doubles data yield a calculated value of $(7.7 \pm 0.9) \times 10^{-4}$ for the "2-D photopeak" efficiency as defined below.

The ^{58}Ni cascade was, in addition, observed in triple coincidence (p-γ-γ). The data are shown in two dimensions in Fig. 5, and a sum projection appears in Fig. 11(a). These spectra, compressed to lower dispersion, were generated off line directly from the original high-dispersion (40 keV/channel) event-recorded data, and include all events whose TAC signal satisfied the triple-real-coincidence requirement. No randoms subtraction was performed, as randoms rates of all types were negligible.

In Fig. 5, tails, largely due to Compton events in one crystal coinciding with full-energy events in the other, extend at right angles from the "2-D photopeaks." The symmetry about the $E_{\gamma_1} = E_{\gamma_2}$ line arises because either γ ray can be detected in either crystal. Figure 6 illustrates that when a *sum* spectrum is formed (either by external analog summing or by projecting 2-D data), a distinction must be made between the "2-D" and the "sum-projection" photopeak efficiencies. The sum-projection photopeak will include additional events that are outside the 2-D photopeaks, and that are not taken into account by using the product of the individual efficiencies to predict the coincidence efficiency. In Fig. 6 the +'s indicate such events. Another consideration is that low-energy thresh-

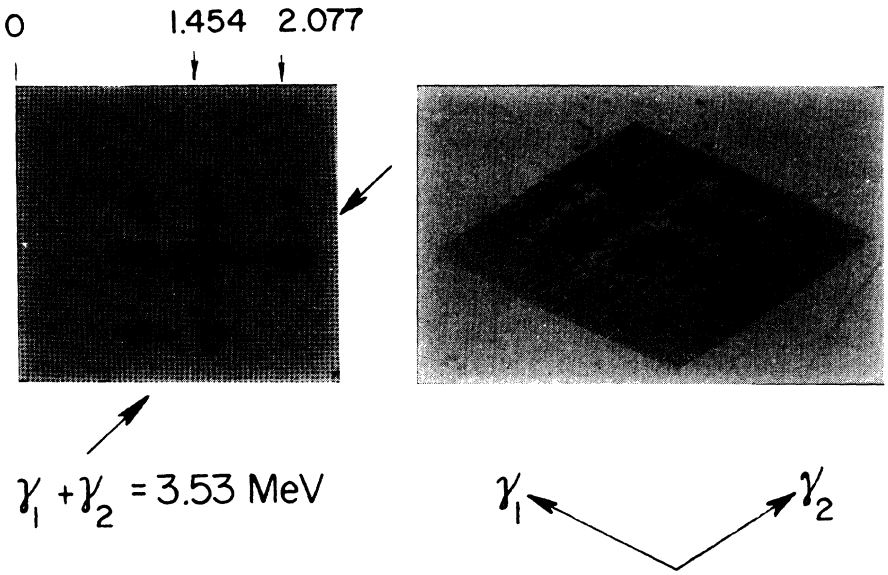

FIG. 5. Triple coincidence data for the 3.53→ 1.46→ 0 $\gamma\gamma$ cascade in ^{58}Ni.

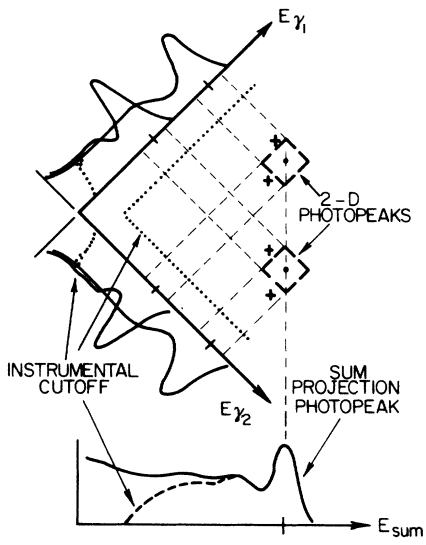

FIG. 6. 2-*D* line shape for a discrete cascade, indicating the distinction between "2-*D*" and "sum-projection" photopeaks. The + 's indicate events not accounted for in a simple-minded calculation of the efficiency.

olds will have a complicated influence on the sum-spectrum line shape. Even when discriminator levels are set quite low for each detector, the effect of the instrumental cutoff can extend to high energies in the sum spectrum, as seen in Fig. 6.

The triples data give a 2-*D* photopeak efficiency of $(7.6 \pm 0.5) \times 10^{-4}$, in good agreement with the doubles prediction, and a sum-projection photopeak efficiency of $(9.1 \pm 0.6) \times 10^{-4}$.

B. Auxiliary γ Measurements on ^{40}Ca

Energy spectra were obtained under a variety of coincidence requirements, in order to investigate possible sources of background and competing processes. γ-ray singles spectra are shown in Fig. 7. Scattered protons which interact in the aluminum chamber walls account for several of the peaks. However, the yield is low compared to the excitation of the state of interest as evidenced by the 0.511-MeV annihilation peak.

Spectra of γ rays in coincidence with protons in the inelastic group of interest, obtained separately for each NaI detector, are shown in Fig. 8(a). The difference in yield of 0.511-MeV γ rays re-

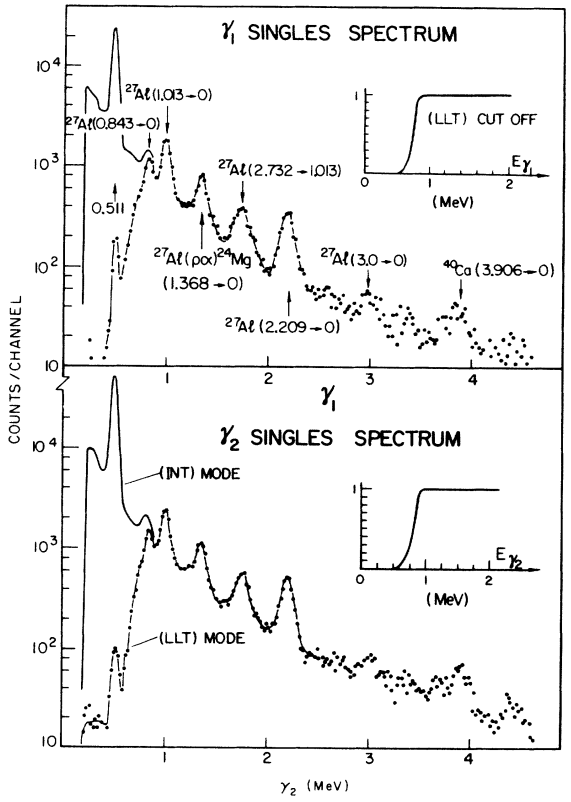

FIG. 7. γ-ray singles spectra for each crystal, as gated by its respective fast discriminator in the internal (INT) and lower-level-timing (LLT) modes, to permit evaluation of the low-energy cutoff.

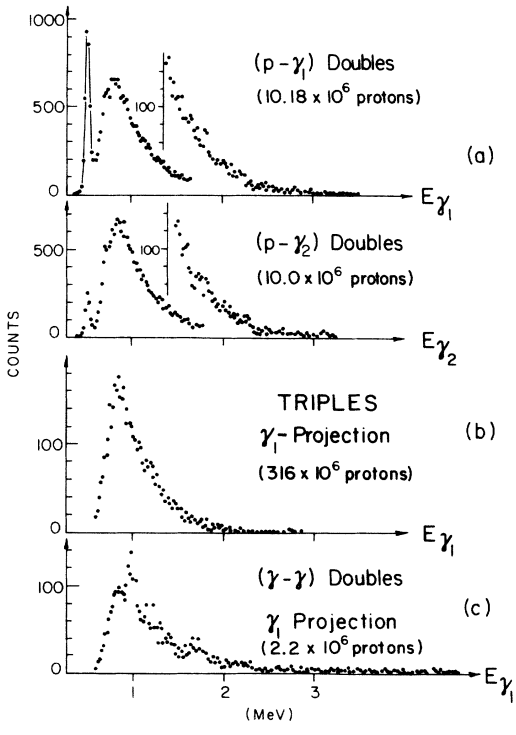

FIG. 8. γ-ray energy spectra in one crystal, under various coincidence conditions. (a) p-γ doubles. (b) Projection on the γ_1 axis of all the ^{40}Ca triples data. (c) Same as (b), for the γ-γ doubles data. The number of proton SCA counts provides normalization.

flects a slight mismatch in fast discriminator thresholds. The spectra exhibit an exponential shape due to bremsstrahlung of the electrons and positrons of the pair decay, and the expected end point of 2.33 MeV is evident. In contrast with the singles data, no peaks are discernible in either p-γ doubles spectrum. The coincidence counting rate was ~3/sec, and the reals-to-randoms ratio was on the order of 80 to 1.

A γ-γ doubles sum projection is seen in Fig. 11. Only the ^{27}Al cascade is evident. Its constituents are seen faintly at 1.0 and 1.7 MeV in the γ_1 projection shown in Fig. 8(c). For this measurement, the coincidence counting rate was also ~3/sec, with a 60 to 1 reals-to-randoms ratio.

A short run was made in triple coincidence with the proton window set just below the 0_2^+-state peak. Only 13 triple real events and seven $\{\gamma[p\gamma]\}$ correlated randoms were observed for a running time of 4.6 h (equivalent to 20×10^6 0_2^+ protons detected). All events but two of the randoms had a sum energy of less than 3 MeV. Finally, a targetless run was made for 0.9 h. No events were observed at all, indicating that nontarget background processes were of no concern.

IV. RESULTS AND ANALYSIS

A. Proton Spectrum

A sample energy spectrum of particles backscattered from the ^{40}Ca target is shown in Fig. 9. Approximately 3% of all counts fall in the region of the peak of interest. Correcting for background, the net number of excitations of the state of interest is given by ~86% of the proton SCA scalar, which experienced an average count rate of ~1.33 $\times10^3$/sec.

B. ^{40}Ca Triples Data

The 2-D spectrum for the ^{40}Ca triples data is shown in Fig. 10. Double γ decay would appear as a ridge along the constant sum-energy locus, as indicated on the figure. There are too few counts for the ridge to be obvious. The sum spectrum for these same data are shown in Fig. 11(e). A photopeak is evident at 3.35 MeV. The rising yield at lower energies is attributed to a variety of bremsstrahlung and annihilation processes associated with the electron-positron pairs of the dominant decay mode. Randoms were not subtracted because of their very low yield. Not a single triple random event was observed in the entire run. Correlated randoms spectra are shown in Figs. 11(c) and 11(d). The $\{p[\gamma\gamma]\}$ type were obtained with a wider TAC window (by a factor of 4.5) than were the triple reals to improve statistical accuracy. The spectrum is reassuringly similar in shape to the γ-γ doubles spectrum. Both types of $\{\gamma[p\gamma]\}$ have been combined and are shown in Fig. 11(d).

These data represent a total of 66 h of running time, during which time the proton SCA registered 3.16×10^8 counts. The total collected charge was 6.65×10^{-3} C, for an average incident beam current of 28 nA. The total triple-coincidence count

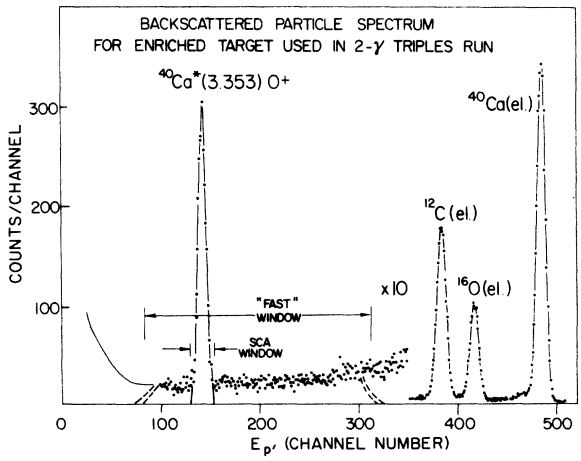

FIG. 9. Typical proton spectrum. The fast discriminator deleted elastics, while the SCA selected the group of interest. The dispersion is 9.5 keV/channel.

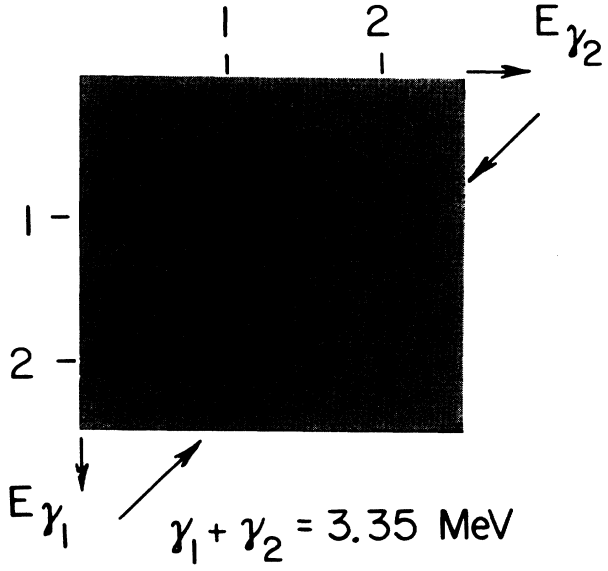

FIG. 10. Two-dimensional (γ_1 vs γ_2) spectrum of the ^{40}Ca triples data. The constant sum locus for double γ decay is indicated.

rate amounted to 2×10^{-2}/sec.

Various projections of the ^{40}Ca data are shown in Figs. 12 and 13. Since the yield for double γ decay is expected to be highest near the center of the sum-energy locus (i.e., for $\mathcal{E}_1 \cong \mathcal{E}_2$), the apparent greater yield in the adjacent regions must be accounted for. In Fig. 13, bands of constant sum energy are projected; the abscissa is $(\mathcal{E}_2 - \mathcal{E}_1)$. In this type of plot, a cascade manifests itself as two symmetric peaks, as evidenced in the ^{58}Ni data which are presented for comparison.

In the calcium data, there is a suggestion of the presence of a cascade at $(\mathcal{E}_2 - \mathcal{E}_1) \approx \pm 0.8$ MeV, but the statistical accuracy is quite low. The data distribution would otherwise seem not to be inconsistent with what would be expected for double γ decay. The dotted line gives the approximate shape for double γ decay of $E1, E1$ multipolarity. A more detailed analysis follows.

C. Maximum-Likelihood Analysis

In order to discern shape information from the experimental yield along the sum locus, a maximum-likelihood technique was used which begins with the determination of an appropriate form for the probability distribution.

The usual assumption for double γ decay between 0^+ states is that of two dipole ($E1$) transitions via virtual excitation of localized high-lying 1^- states. This leads to the following expression for the (normalized) energy distribution of either of the γ rays:

$$P_{2\gamma}(\mathcal{E}_1)d\mathcal{E}_1 = \frac{140}{\mathcal{E}_0^{\,7}}\mathcal{E}_1^{\,3}(\mathcal{E}_0 - \mathcal{E}_1)^3 d\mathcal{E}_1 ,$$

where $\mathcal{E}_1$ is the energy of one of the γ rays and $\mathcal{E}_0$ is the sum energy. A change of variables can be made, defining $x = (\mathcal{E}_2 - \mathcal{E}_1)$:

$$P^{(0)}_{2\gamma}(x)dx = \frac{1}{\mathcal{E}_0^{\,7}}\frac{35}{32}(\mathcal{E}_0^{\,2} - x^2)^3 dx ,$$

$$\mathcal{E}_1 = \frac{\mathcal{E}_0 - x}{2}, \quad \mathcal{E}_2 = \frac{\mathcal{E}_0 + x}{2}.$$

This function, normalized to the total number of counts, is the dotted line plotted in Fig. 13 and also appears in Fig. 14(a).

Two instrumental effects must be taken into account. First, since yield is expected along the entire sum-energy locus, a correction was made for the low-energy thresholds, as indicated in Figs.

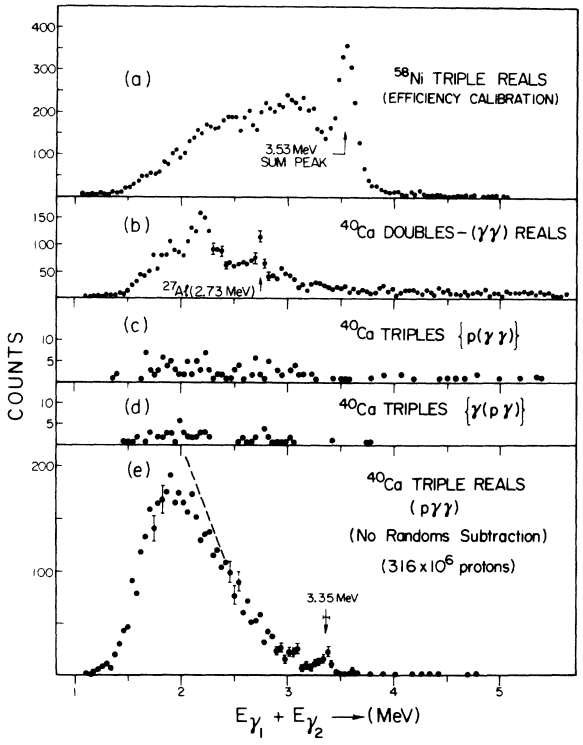

FIG. 11. γ-γ sum projections.

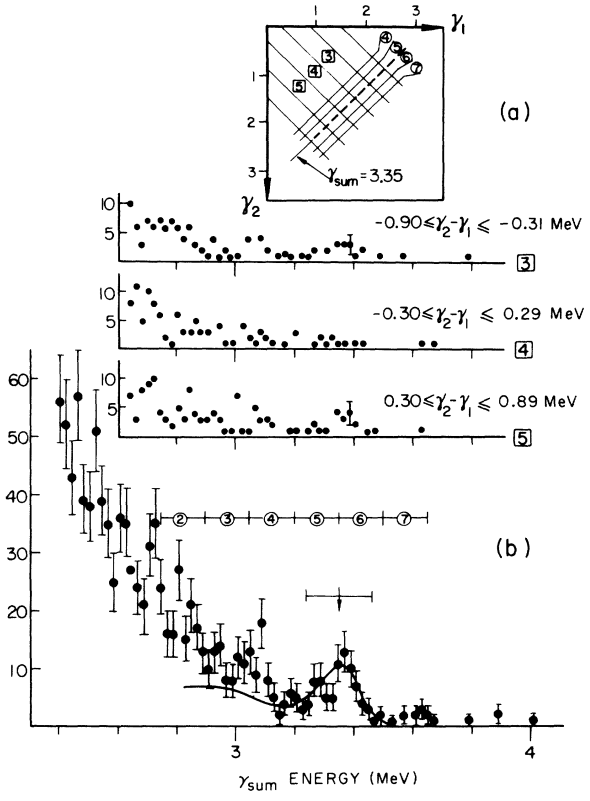

FIG. 12. (a) The regions of the triples 2-D spectrum indicated are projected in (b) and Fig. 13. (b) Subsets of the sum projection are labeled in (a) by the numbered sqaures. The bottom graph shows an expanded view of the total sum projection.

7 and 14(c). Second, the triples efficiency is a function of $\mathcal{E}_1$ and $\mathcal{E}_2$, or equivalently x and $\mathcal{E}_0$, and will vary along the ^{40}Ca sum-energy locus. Tabulated[32] efficiency values for each crystal were presumed adequate to compute the *relative* triples efficiency, defined for convenience with respect to the value at $\mathcal{E}_1 = \mathcal{E}_2 = 1.67$ MeV ($x = 0$, $\mathcal{E}_0 = 3.35$ MeV):

$$a_{\mathcal{E}_0}(x) = \frac{2\epsilon(\mathcal{E}_1)\epsilon(\mathcal{E}_2)}{2\epsilon(1.67)\epsilon(1.67)},$$

where $\epsilon(\mathcal{E})$ is the photopeak efficiency for one crystal.

The function $a(x)$, shown in Fig. 14(b), provided sufficient information for analysis of the spectrum shape, but to obtain a value for the branching ratio the efficiency measured in the ^{58}Ni run required suitable normalization.

Combining these effects, a shape $P_{2\gamma}(x)$, shown in Fig. 14(d), was predicted for the projected spectrum of double γ decay events. To check for the presence of a cascade, symmetrically placed peaks were added to the trial function $P_{2\gamma}(x)$. The position and area of these peaks were varied to search for a maximum-likelihood solution (for Poisson statistics).[33] The total trial function was normalized to the total number of counts in the data. The resultant best-fit function shown in Fig. 14(e) had 9 counts in each peak, with the peaks placed at ±10 channels from the center ($x = \pm 0.8$ MeV). This result was insensitive to the width used for the peaks, although, by varying the width, a shallow maximum in the likelihood was found for a full width at half maximum (FWHM) of 0.16 MeV, in agreement with the ^{58}Ni peak widths as observed in the $(\mathcal{E}_2 - \mathcal{E}_1)$ projection. Attempts to give the two peaks unequal numbers of counts led to a lower likelihood. Figure 15(a) shows the likelihood values obtained.

If, in this application, the maximum-likelihood technique has validity, it must be capable of determining the parameters of the parent distribution from a sample having low statistical accuracy. Using the "best-fit" trial function obtained above as a parent probability distribution, simulated spectra, each having 88 counts, were generated by a Monte Carlo technique. Each simulation was then fitted by maximum likelihood to recover its "known" parameter set. The results for extraction of the number of counts in the cascade peaks are shown in Fig. 15(b); peak position was fitted equally well. It is apparent that for each simulation, the technique had sufficient sensitivity to ex-

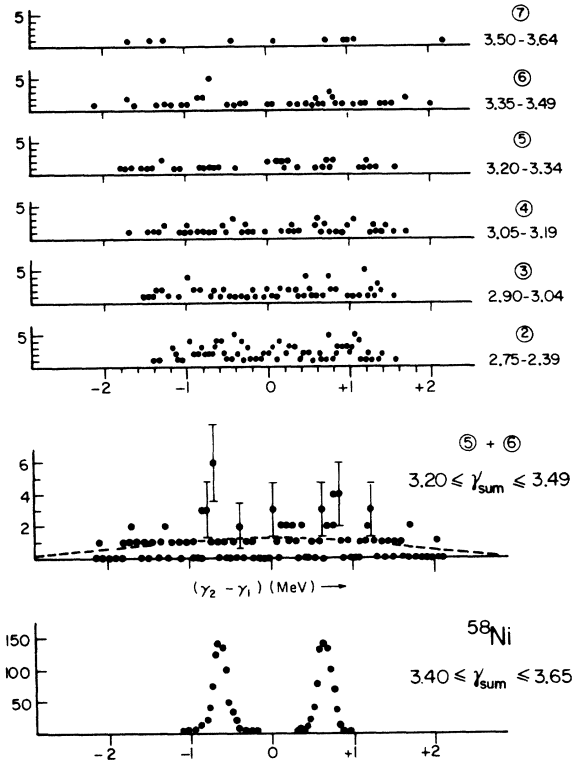

FIG. 13. Projections of regions labeled by the numbered circles in Fig. 12(a).

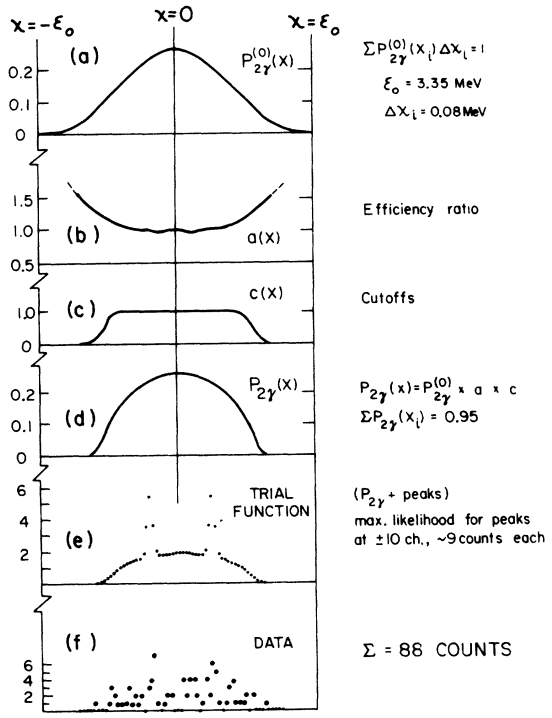

FIG. 14. (a)–(d) Derivation of the parent probability distribution for 2-γ decay. (e) Trial function which best fits the data, which is shown again in (f).

tract the parameters, within error bars. The distribution of actual values of the maximum likelihood, shown in Fig. 15(c), is reasonably clustered, and the value for the data does fall within range.

In a final test, the likelihood of the data was calculated for functions consisting of two peaks and slight variants of $P_{2\gamma}(x)$, obtained by making small changes in the coefficients of a polynominal fit to $P_{2\gamma}(x)$. No substantially higher likelihood was found than the value $W^{\mathrm{DATA}} = -82.0$ reported in Fig. 15.

Although events are observed at energies greater than 3.5 MeV in the sum projection [Fig. 12(b)], there is no obvious reason to assume that the process giving rise to these counts would make an equivalent background contribution to the photopeak region. Therefore, no background was subtracted. However, the error on the number of photopeak events was estimated to reflect a possible background contribution of 15 counts. Of the 88 counts in the sum photopeak, 18 ± 6 are attributed to an extraneous cascade, and 70^{+10}_{-25} are then presumed to be due to double γ decay.

D. Branching Ratio

For a given value of the branching ratio, $R = \Gamma_{\gamma\gamma}/\Gamma$, the number of counts n_i expected in channel i of width Δx_i is given by:

$$n_i = R N_p W(\theta) \mathcal{P}_i ,$$

$$\mathcal{P}_i = P_{2\gamma}(x_i)\Delta x_i \frac{\mathrm{Effic(Ni)}}{a\mathrm{(Ni)}} ,$$

$$a\mathrm{(Ni)} = \frac{\epsilon(1.45)\epsilon(2.07)}{\epsilon(1.67)\epsilon(1.67)} = 0.92 ,$$

where N_p is the net number of protons. $\mathcal{P}_i$ is the total absolute probability of detecting a double γ-decay event in channel i, and the measured sum peak efficiency has been normalized appropriately. $W(\theta)$ is the angular-correlation correction for a $0 \to 1 \to 0$ cascade.

Summing both sides of the above expression over all channels, the branching ratio is given by:

$$R = \frac{\text{No. of } 2\gamma \text{ events}}{N_p W(\theta)[\mathrm{Effic(Ni)}/a\mathrm{(Ni)}]\sum_i P_{2\gamma}(x_i)\Delta x_i} ,$$

$$\sum_i P_{2\gamma}(x_i) dx_i = 0.95 ,$$

$$W(\theta) = 0.83 ,$$

$$N_p = 2.72 \times 10^8 ,$$

$$\mathrm{Effic\,(Ni)} = (9.1 \pm 0.6) \times 10^{-4} ,$$

$$\text{No. of } 2\gamma \text{ events} = 70^{+10}_{-25} \text{ counts} ,$$

$$\Gamma_{\gamma\gamma}/\Gamma = (3.3^{+0.5}_{-1.2}) \times 10^{-4} .$$

V. DISCUSSION

A. Background Considerations

If a significant amount of ^{42}Ca or ^{44}Ca were present in the target, states in these nuclei would have contributed strongly to the observed coincidence spectrum, since each isotope has states near 3.35 MeV as well as intermediate states to permit cascades.

Auxiliary measurements were made of the particle spectra for various calcium targets. Inelastic scattering yields, together with the known isotopic abundances of the various targets, enable upper limits to be calculated for the ^{42}Ca and ^{44}Ca contributions to the ^{40}Ca sum-coincidence γ spectrum. The yields from the 3.19- and 3.44-MeV states in ^{42}Ca were found to be completely negligible, and the 3.30-MeV state in ^{44}Ca was found to contribute <1 count. As a further precaution, the yields from the states in ^{42,44}Ca were checked for resonant behavior over the region of the resonance at 5.08 MeV populating the 0_2^+ state in ^{40}Ca. No significant variations in yield were found.

It should be noted that the large accumulated incident beam, and the low number of observed

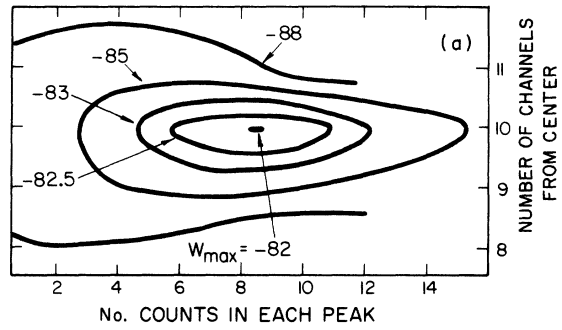

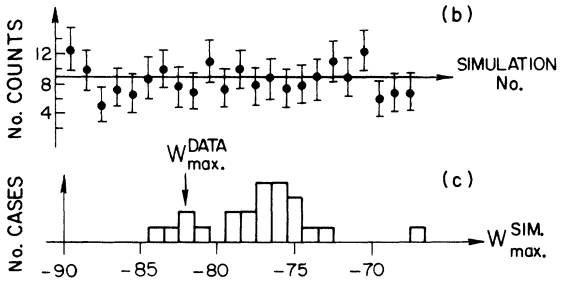

FIG. 15. (a) Contours of $W = \ln L$ (L is the likelihood) for grid search of fitting parameters. (b) Parameter values extracted from each simulated spectrum, where the "known" value was 9 counts. (c) Histogram of likelihoods obtained in fitting the simulated spectra.

events, makes this experiment sensitive to the presence of a very small amount of a target impurity, assuming a reasonable reaction cross section. For example, both ^{18}F and ^{38}Ar have excited states near 3.35 MeV and intermediate states which would account for the discrete γ-γ cascade observed. However, these states can be reached only by reactions on extremely unlikely target impurities, ^{21}Ne$(p,\alpha)^{18}$F and ^{41}K(p,α)Ar.

For (p,p') reactions, the discrimination of the particle energy window is not as thorough as might be expected. Taking into account the range of γ-sum energies that was allowed, and the actual proton-energy-window width of 220 keV, reactions (to states at 3.2–3.5 MeV in excitation) on targets with mass between 20 and 200 amu can kinematically meet the requirement. But while one such case might account for the weak cascade which seems to be present in the data, it is unlikely that the target contained a collection of impurities, all of the same "abundance $\times$ cross section," and with appropriate cascade decays, to account for the continuum yield that was observed.

In view of the experimental technique used (triple coincidence with proton energy selection), it is conceivable that a γ cascade could proceed in the compound nucleus ^{41}Sc, followed by emission of a proton with the same energy as the inelastically scattered proton from the 3.35-MeV state. Since the particle energy is selected in each event, exactly the desired remaining energy, 3.35 MeV, is available to radiative transitions. Whether the proton or the γ rays are emitted first was not distinguished in the measurement. The dotted line in Fig. 1 indicates such a process. Proton decay of states at 2.66 or 2.71 MeV in ^{41}Sc to the ground state of ^{40}Ca would give protons of about the right energy. However, since all of the many intermediate states[25,34,35] are particle unstable, they have very small γ-decay probabilities. Measured total widths, single-particle γ-decay widths, and values of maximum known enhancements,[36] have been used to calculate a typical probability for this process. The result is 6×10^{-8} for the particular case of a $(M1,E1)$ cascade through the $\frac{1}{2}^+$ state at 3.966 MeV. No other choice of intermediate state, or multipolarities, will lead to a significantly larger number. This process, therefore, obviously cannot account for either the continuous yield or the faint peaks, by a factor of 10^3 or more. Very large enhancements of γ widths, or an as yet unknown state in ^{41}Sc having a very narrow particle width, would be needed. Both of these possibilities are very unlikely, though not impossible.

The dominant decay mode of the state of interest is by electron-positron pair emission. For a given decay, each particle may have a kinetic energy ranging from 0 to 2.33 MeV, and their energies must add to 2.33 MeV. Any process by which these particles can have their energies converted to photons is of concern because such events will be in real coincidence with inelastic protons in the "window."

One can imagine several such processes, but only a few have the capability of depositing, in the two crystals, a γ-sum energy greater than 2.33 MeV, much less approaching 3.35 MeV. The most probable of the full-energy processes involves a positron, emitted at nearly the full 2.33-MeV kinetic energy, which annihilates in flight in the region of the target. However, this could account for at most a few counts in the region of the 3.35-MeV sum peak. Furthermore, owing to the energy asymmetry of photons emitted by annihilation in flight, such events would be least likely at $\mathcal{E}_2 - \mathcal{E}_1 \simeq 0$.

It should be emphasized that no such process can account for a sum photopeak, since they all involve probabilities which decrease exponentially to zero at the energy endpoint. A variety of other multiple processes have been considered (including "internal" bremsstrahlung), but rejected due to very low probability and/or lower energy endpoints (due to the escape of one or more annihilation quanta).

Many possible auxiliary measurements suggest themselves in the attempt to find explanations other than double-photon decay for the observed γ coincidence yield. Harihar, Ullman, and Wu[22] examined the coincidence yield for incident beam energies on and off resonance, in the hope that effects other than double-photon decay might be accounted for. This might be partially useful for investigating target impurities (presuming that excited states in the impurities are not resonantly populated) but it specifically does not examine processes associated with the pair decay (quite simply, the state in ^{40}Ca is not populated as often) which dominate the low-energy portion of the spectrum. In particular, detector singles count rates must change considerably, since the yield of 0.511-MeV annihilation quanta will change, thus affecting pileup, dead time, and the reals-to-randoms ratio. Also, an off-resonance measurement by definition cannot examine the possibility of decay in the compound nucleus, as discussed above.

The probability of only one γ ray being emitted prior to proton decay of the compound system (to the ground states of ^{40}Ca) is much higher than for a γ cascade. This process, $(p,\gamma p')$, could be seen as a γ ray in coincidence with protons having recoil energy commensurately above that of the protons from the 0^+ excited state in ^{40}Ca. Therefore a run with the proton window set differently could

check on at least part of this process, as well as other completely unexpected or obscure effects.

B. Theoretical Considerations

Extraction of a value for the branching ratio from the data is dependent on several theoretical assumptions. The most basic is that a second-order perturbation-theory derivation can be used, and that several terms arising therein may be neglected. The use of perturbation theory itself may deserve further scrutiny.[37-39] The dipole approximation is usually made, which for 0^+-0^+ transitions in self-conjugate nuclei implies that in the sum over intermediate states one need consider only 1^- $T=1$ states. This immediately assures $(E1, E1)$ multipolarities and fixes the $\gamma\gamma$ angular correlation as $(1+\cos^2\theta)$. Furthermore, such 1^- states are generally localized in the giant dipole resonance, permitting approximations which lead to the continuum energy distribution used above (see for example Ref. 12).

Before meaningful use can be made of nuclear-model estimates, however, questions on the validity of expressions to be used must be resolved. For example, discrepancies among different authors are evident as to multiplicative factors, depending on what simplifications are attempted and assumptions made. [For example, compare Eq. (18), Ref. 40, with Refs. 5, 19, and 41.]

"Single-particle" estimates of double γ decay are usually of the order of 10^{-2}. Such estimates are not to be taken seriously, as nuclear excited states are known to be of a more complex nature, often involving excitation of more than one particle, or collective motion.

Several years ago, in the first attempt at a detailed nuclear-structure calculation of double γ decay, Bertsch[42] obtained for the case of ^{16}O a theoretical branching ratio just below the experimental limit. However, a recent effort[43] to make a more general detailed calculation for ^{16}O, ^{40}Ca, and ^{90}Zr provided qualitative understanding of the smallness of the branch but not quantitative agreement with experiment. In each nucleus, the two 0^+ states involved are assumed to have only a spherical and a deformed component, and the 2γ transition operator is taken to be of the second-order $E1$ form. Neglecting cross terms (arguing that they are small), two diagonal intrinsic matrix elements remain. Using the geometrical properties of the spherical and deformed components of the dipole state, each term is then evaluated with the dipole sum rule.

This treatment of the nuclear structure is highly schematic. The 0^+ ground state, and first excited state, in both ^{16}O and ^{40}Ca, are generally held to be well described by superpositions of (0p-0h), (2p-2h), and (4p-4h) intrinsic 0^+ shell-model wave functions (for example see Ref. 44). The use of a simplified model for these states is mitigated somewhat by using the empirical monopole matrix element to fix the admixture coefficients, but the use of the sum rule and neglect of cross terms may or may not prove adequate. If, for example, the more detailed model is used for the 0^+ states, cross terms of the form $\langle 0\text{p-}0\text{h}|M|2\text{p-}2\text{h}\rangle$ might be considered. Recent calculations[45] in ^{16}O have met success by interpreting the intermediate structure in the giant resonance in terms of (3p-3h) states coupled to (1p-1h) states. This could make possible nonzero terms of the type $\langle 2\text{p-}2\text{h}|M|4\text{p-}4\text{h}\rangle$.

C. Conclusions

A positive indication of double γ decay may have been observed from the first excited state in ^{40}Ca (0^+, 3.35 MeV), which normally decays by $E0$ monopole pair emission. The indicated double γ-decay branching ratio obtained in the present experiment is $\Gamma_{\gamma\gamma}/\Gamma = (3.3^{+0.5}_{-1.2}) \times 10^{-4}$, somewhat below the last reported upper limit.

To permit the effect to be seen, background in the measured spectrum was minimized by the imposition of a fast-triple-coincidence requirement, suitable shielding, and by the use of a very pure target. A separate efficiency-calibration measurement and extensive monitoring of the electronics system, together with a number of auxiliary background measurements under different coincidence conditions, have increased confidence in the result. High-dispersion multidimensional event recording permitted subsequent analysis of the shape of the continuous spectrum, which was found to be consistent with the theoretically pre-$E1, E1$ multipolarities.

A measured value of the double γ-decay branching ratio does provide new information about the states involved. However, its usefulness in testing theories of the structure of nuclear states is hampered by the uncertainties in how to deal with the process itself, and the difficulty of separating the formalism for calculations from the nuclear structure to be put into them. Recent theoretical calculations, though preliminary, would not seem inconsistent with the present finding. The fate of previous experiments claiming to observe double γ decay serves as a warning on presuming the issue closed, experimentally or theoretically.

ACKNOWLEDGMENTS

The authors thank D. H. Wilkinson for providing initial inspiration and continued interest. We further thank G. Bertsch, D. Harrington, and L. Zam-

ick for many enlightening discussions. We acknowledge and greatly appreciate the participation in the data taking by Y. Hashimoto and J. Matthews. We express gratitude to M. Robbins for writing the data-taking computer program, to M. Ulrickson for assistance in the analysis, and particularly to R. Klein for the preparation of the targets.

---

†Work supported in part by the National Science Foundation.
*Ph.D. thesis, Rutgers University, June 1972; present address: Brookhaven National Laboratory, Upton, New York 11973.
‡Present address: Department of Physics, University of Washington, Seattle, Washington 98105.
§Present address: Victoria University of Wellington, Wellington, New Zealand.
¶Associate of the graduate faculty, Rutgers University.

[1]M. Goeppert-Mayer, Ann. Phys. (Leipz.) **9**, 273 (1931). Translation available from the National Translation Center, Chicago, Ill.
[2]G. Breit and E. Teller, Astrophys. J. **91**, 215 (1940).
[3]V. W. Hughes and J. S. Geiger, Phys. Rev. **99**, 1842 (1955), and references therein.
[4]R. C. Elton, L. J. Palumbo, and H. R. Greim, Phys. Rev. Lett. **20**, 783 (1968). Also see R. W. Schmeider and R. Marrus, Phys. Rev. Lett. **25**, 1692 (1970).
[5]J. R. Oppenheimer and J. S. Schwinger, Phys. Rev. **56**, 1066 (1939).
[6]R. G. Sachs, Phys. Rev. **57**, 194 (1940).
[7]J. C. Vanderleeden and P. S. Jastram, Phys. Rev. C **1**, 1025 (1970).
[8]T. Alväger and H. Ryde, Ark. Fys. **17**, 535 (1960). Also Phys. Rev. Lett. **4**, 363 (1960).
[9]H. J. Fischbeck and A. A. Abdulla, in *Proceedings of the International Conference on Electron Capture and Higher-Order Processes in Nuclear Decay, Debrecen, Hungary, 15–18, July, 1968*, edited by D. Berényi (Eötvos Lóránd Physical Society, Budapest, Hungary, 1968).
[10]W. Beusch, Helv. Phys. Acta **33**, 362 (1960).
[11]A. Schwarzschild, private communication; Brookhaven National Laboratory Progress Report, July 1, 1959 (unpublished).
[12]G. F. Dell, P. S. Jastram, and H. J. Hausman, Bull. Am. Phys. Soc. **6**, 93 (1961).
[13]S. Gorodetzky, G. Sutter, R. Armbruster, P. Chevallier, P. Menrath, F. Scheibling, and J. Yoccoz, J. Phys. Radium **22**, 688 (1961).
[14]S. Gorodetzky, G. Sutter, R. Armbruster, P. Chevallier, P. Menrath, F. Scheibling, and J. Yoccoz, Phys. Rev. Lett. **7**, 170 (1961).
[15]H. Langhoff and H. H. Hennies, Z. Phys. **164**, 166 (1961).
[16]H. Ryde, P. Thieberger, and T. Alväger, Phys. Rev. Lett. **6**, 475 (1961).
[17]M. Nessin, T. H. Kruse, and K. W. Eklund, Phys. Rev. **125**, 639 (1962).
[18]H. Ryde, Ark. Fys. **23**, 247 (1963).
[19]G. Sutter, Ann. Phys. (Paris) **8**, 323 (1963).
[20]D. E. Alburger and P. Parker, Phys. Rev. **135**, B294 (1964).
[21]J. C. Vanderleeden and P. S. Jastram, Phys. Lett. **19**, 27 (1965).
[22]P. Harihar, J. D. Ullman, and C. S. Wu, Phys. Rev. C **2**, 462 (1970).
[23]Y. Nakayama, Phys. Rev. C **7**, 322 (1973).
[24]R. D. Bent and T. H. Kruse, Phys. Rev. **109**, 1240 (1958).
[25]A. Marinov, Ch. Drory, E. Navon, J. Burde, and G. Engler, Nucl. Phys. **A145**, 534 (1970).
[26]I. S. Sherman, R. G. Roddick, and A. J. Metz, IEEE Trans. Nucl. Sci. **NS-15**, 500 (1968).
[27]Designed and built at Bell Telephone Laboratories.
[28]E. A. Gere and H. P. Lie, IEEE Trans. Nucl. Sci. **NS-16**, 436 (1968).
[29]E. A. Gere and G. L. Miller, IEEE Trans. Nucl. Sci. **NS-13**, 508 (1965).
[30]E. A. Gere, H. P. Lie, G. L. Miller, and A. Senator, IEEE Trans. Nucl. Sci. **NS-17**, 436 (1970).
[31]D. F. H. Start, R. Anderson, L. E. Carlson, A. G. Robertson, and M. A. Grace, Nucl. Phys. **A162**, 49 (1971).
[32]J. B. Marion and F. C. Young, *Nuclear Reaction Analysis—Graphs and Tables* (North-Holland, Amsterdam; Wiley, New York, 1968).
[33]E. Beardsworth and M. Ulrickson, Bull. Am. Phys. Soc. **17**, 893 (1972).
[34]D. H. Youngblood, B. H. Wildenthal, and C. M. Class, Phys. Rev. **169**, 859 (1968).
[35]P. M. Endt and C. Van Der Leun, Nucl. Phys. **A105** (1967).
[36]S. J. Skorkas, J. Hertel, and T. W. Retz-Schmidt, Nucl. Data **A2**, 347 (1966).
[37]E. J. Hellund, Phys. Rev. **89**, 919 (1953).
[38]M. Namiki and N. Mugibayashi, Prog. Theor. Phys. **10**, 474 (1953).
[39]N. Friedman, IBM Report No. RC 3596, 1971 (unpublished). Also Bull. Am. Phys. Soc. **17**, 564 (1972), and private communication.
[40]D. P. Grechukin, Nucl. Phys. **62**, 273 (1965). See also Zh. Eksp. Teor. Fiz. **32**, 1036 (1957) [transl.: Sov. Phys.-JETP **5**, 846 (1957)]; Nucl. Phys. **35**, 98 (1962); Nucl. Phys. **47**, 273 (1963); Yad. Fiz. **4**, 42 (1966) [transl.: Sov. J. Nucl. Phys. **4**, 30 (1967)].
[41]B. Margolis, Nucl. Phys. **28**, 524 (1961).
[42]G. F. Bertsch, Phys. Lett. **21**, 70 (1966).
[43]G. F. Bertsch, private communication (to be published in Particles and Nuclei).
[44]R. A. Broglia, K. Kollveit, and B. Nilsson, Phys. Lett. **37B**, 441 (1971).
[45]C. M. Shakin and W. L. Wang, Phys. Rev. Lett. **26**, 902 (1971).

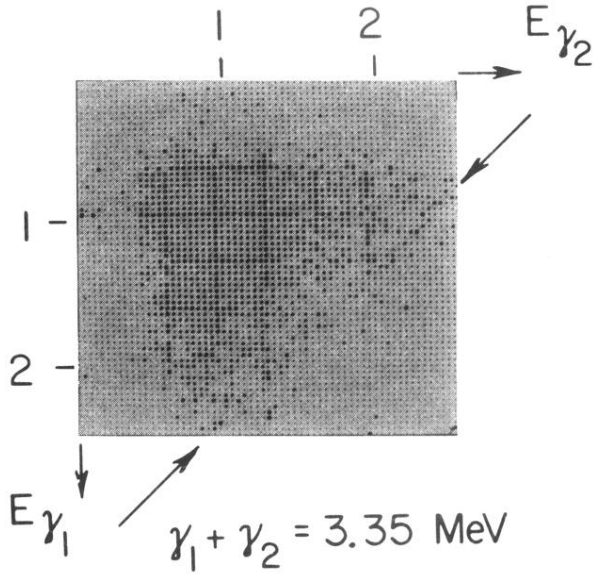

FIG. 10. Two-dimensional (γ_1 vs γ_2) spectrum of the ^{40}Ca triples data. The constant sum locus for double γ decay is indicated.

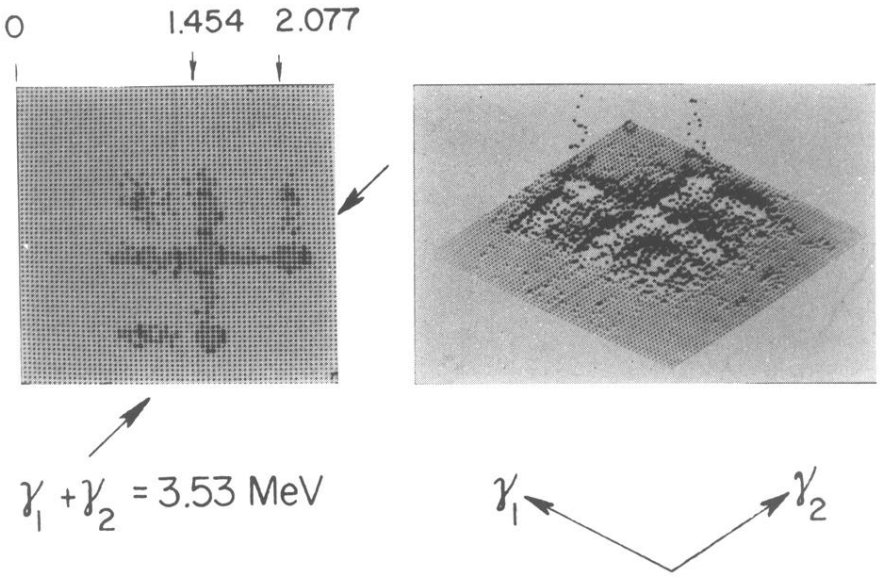

FIG. 5. Triple coincidence data for the $3.53 \rightarrow 1.46 \rightarrow 0$ $\gamma\gamma$ cascade in ^{58}Ni.